Shuvankar Mandal, Suraj Mondal, Cyril Rajnák, Ján Titiš, Roman Boča, Sasankasekhar Mohanta

Electronic Supplementary Information

Table S1 Crystallographic data for **1** and **2**

Compound	**1**	**2**
Formula	$C_{22}H_{39}N_{16}O_2Co_2$	$C_{23}H_{41}N_{16}O_2Co_2$
Formula weight	677.55	691.58
Crystal system	orthorhombic	orthorhombic
Space group	$P2_12_12_1$	$P2_12_12_1$
a /Å	8.424(6)	8.6745(14)
b /Å	13.764(9)	13.701(2)
c /Å	25.759(16)	26.368(4)
α /°	90	90
β /°	90	90
γ /°	90	90
V /Å^3	2987(3)	3133.9(9)
Z	4	4
Temperature /K	296(2)	296(2)
2θ /°	3.16 – 51.19	3.09 –50.32
μ /mm^{-1}	1.162	1.109
ρ_{calcd} /g cm^{-3}	1.507	1.466
F(000)	1412	1444
Absorption-correction	Multi−scan	Multi−scan
Index ranges	$-9 \le h \le 10$	$-8 \le h \le 10$
	$-16 \le k \le 16$	$-16 \le k \le 16$
	$-30 \le l \le 31$	$-31 \le l \le 31$
Reflections collected	14078	21853
Independent reflections	5331	5592
R_{int}	0.1148	0.0510
R_1[a], wR_2[b] [I > 2σ(I)]	0.0797, 0.1745	0.0484, 0.1308
R_1[a], wR_2[b] (for all F_o^2)	0.1673, 0.2173	0.0595, 0.1387

[a] $R_1 = [\sum||F_o| - |F_c||/\sum|F_o|]$. [b] $wR_2 = [\sum w(F_o^2 - F_c^2)^2/\sum w(F_o^2)^2]^{1/2}$.

Table S2 Selected bond lengths (Å) and angles (deg) in **1** and **2**

	1	**2**
	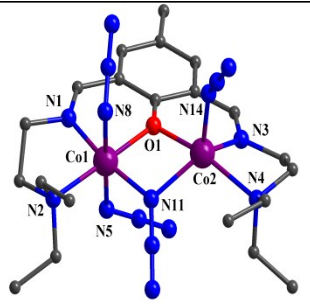	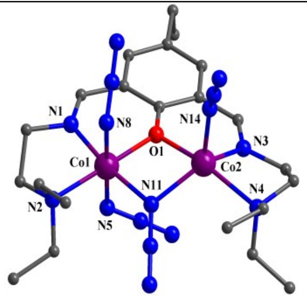
Co1−O1	1.910(9)	1.910(4)
Co1−N1	1.874(12)	1.885(6)
Co1−N2	2.041(12)	2.082(6)
Co1−N5	1.952(13)	1.948(6)
Co1−N8	1.952(12)	1.959(6)
Co1−N11	1.962(15)	2.009(6)
Co2−O1	**2.099(10)**	**2.127(4)**
Co2−N3	**1.984(13)**	**2.020(6)**
Co2−N4	**2.188(14)**	**2.222(6)**
Co2−N11	**2.039(15)**	**2.063(6)**
Co2−N14	**1.998(17)**	**1.983(9)**
O1−Co1−N2	179.6(5)	179.1(2)
N1−Co1−N11	171.9(6)	172.4(2)
N5−Co1−N8	178.2(5)	178.2(3)
O1−Co1−N1	92.5(5)	92.5(2)
N1−Co1−N2	87.1(6)	86.6(2)
N2−Co1−N11	101.0(6)	100.9(2)
N11−Co1−O1	79.3(5)	80.0(2)
N5−Co1−O1	90.6(5)	90.3(2)
N5−Co1−N1	89.9(5)	89.5(2)
N5−Co1−N2	89.5(5)	89.2(2)
N5−Co1−N11	90.3(6)	92.0(3)
N8−Co1−O1	87.6(4)	88.3(2)
N8−Co1−N1	89.8(6)	89.4(3)
N8−Co1−N2	92.2(5)	92.1(2)
N8−Co1−N11	89.7(6)	88.9(3)
O1−Co2−N4	159.7(5)	158.8(2)
N3−Co2−N11	136.7(5)	136.8(3)
O1−Co2−N3	85.8(5)	85.7(2)
N3−Co2−N4	81.8(5)	81.3(2)
N4−Co2−N11	105.4(6)	104.7(2)
N11−Co2−O1	73.3(5)	73.9(2)
N14−Co2−O1	98.9(6)	99.7(3)
N14−Co2−N3	106.8(6)	104.7(3)
N14−Co2−N4	100.0(7)	99.8(3)
N14−Co2−N11	113.5(6)	115.9(3)
Co1−N11−Co2	102.5(7)	101.2(3)
Co1−O1−Co2	102.1(5)	102.27(19)

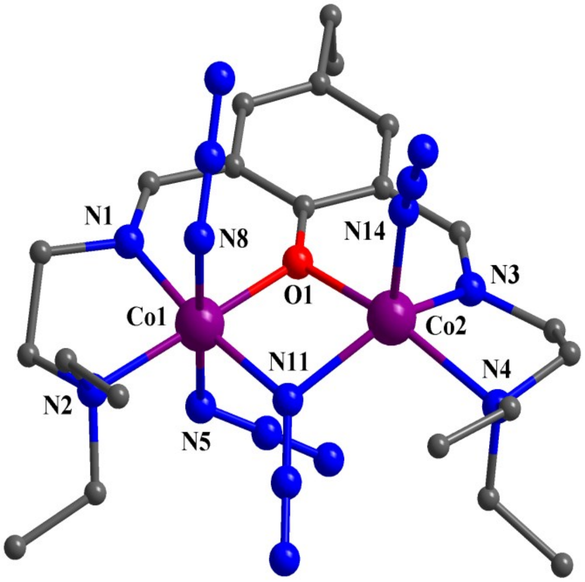

Fig. S1 Crystal structure of $[Co^{III}(N_3)_2L^2(\mu_{1,1}\text{-}N_3)Co^{II}(N_3)]\cdot MeOH$ (**2**). Methanol molecule and hydrogen atoms are omitted for clarity.

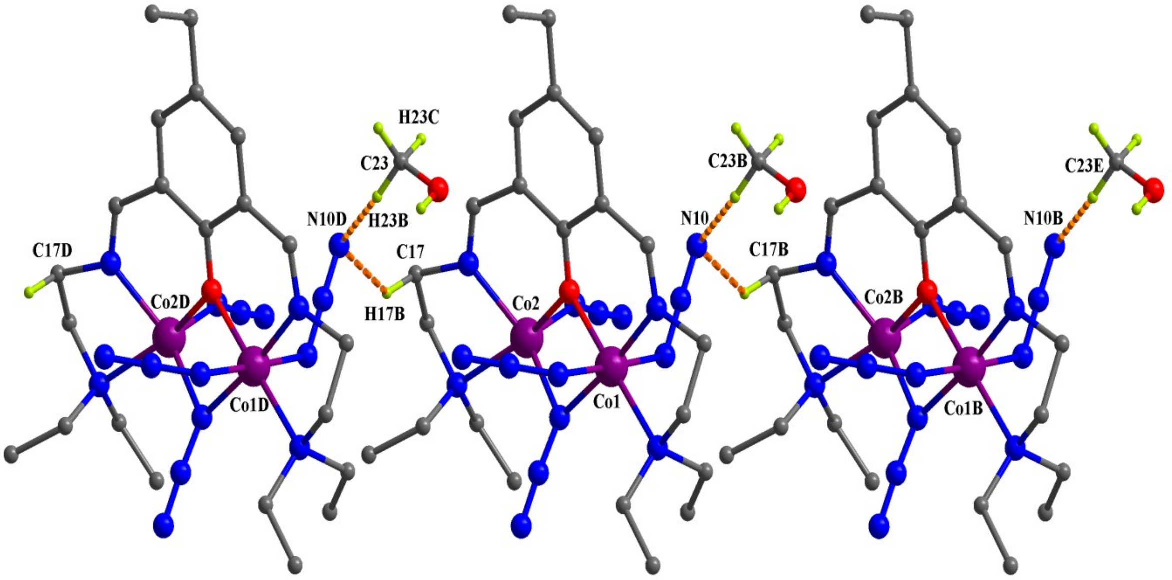

Fig. S2 Perspective view of $[Co^{III}(N_3)_2L^2(\mu_{1,1}\text{-}N_3)Co^{II}(N_3)]\cdot MeOH$ (**2**) showing the one-dimensional ladder topology. Hydrogen atoms, except those participating in the hydrogen bonds and hydrogen atoms in methanol molecules, are omitted for clarity. Symmetry codes: B, –1+*x*, *y*, *z*; D, 1+*x*, *y*, *z*; E, –2+*x*, *y*, *z*.

Table S3 Geometries (distances in (Å) and angles in (°) of the hydrogen bonds in **1** and **2**. [a]

Compound	D–H···A	D···A	H···A	D–H···A
1	C(22)–H(22A)···N(10D)	2.906	2.109	139.54
	C(16)–H(16B)··· N(10D)	3.289	2.561	132.17
2	C(23)–H(23B)···N(10D)	2.845	1.949	154.19
	C(17)–H(17B)··· N(10D)	3.305	2.578	131.80

[a] Symmetry D, –1+*x*, *y* for **1** and 1+*x*, *y*, *z* for **2**.

Table S4 The lowest energy levels (cm^{-1}) and spin Hamiltonian parameters for **2** by *ab initio* (ORCA) calculations.

Property	**2**
Quartet excitation energy (NEVPT2) from $^4A_1$ ground term	
1	1245
2	2349
3	2842
4	5545
5	8129
6	10510
7	22051
8	22077
9	23187
g_1	1.990
g_2	2.355
g_3	2.543
g_{iso}	2.296
D /cm^{-1}	45.7
E/D	0.19
Principal contributions to D from quartet excitation	
1	12.9
2	0.2
3	22.1
4	8.0
Kramers doublet E_i [a]	
2	96.5
3	1568
4	1806
5	3308
6	3410

[a] The lowest spin-orbit corrected energies (first Kramers doublet at zero).

AC susceptibility data

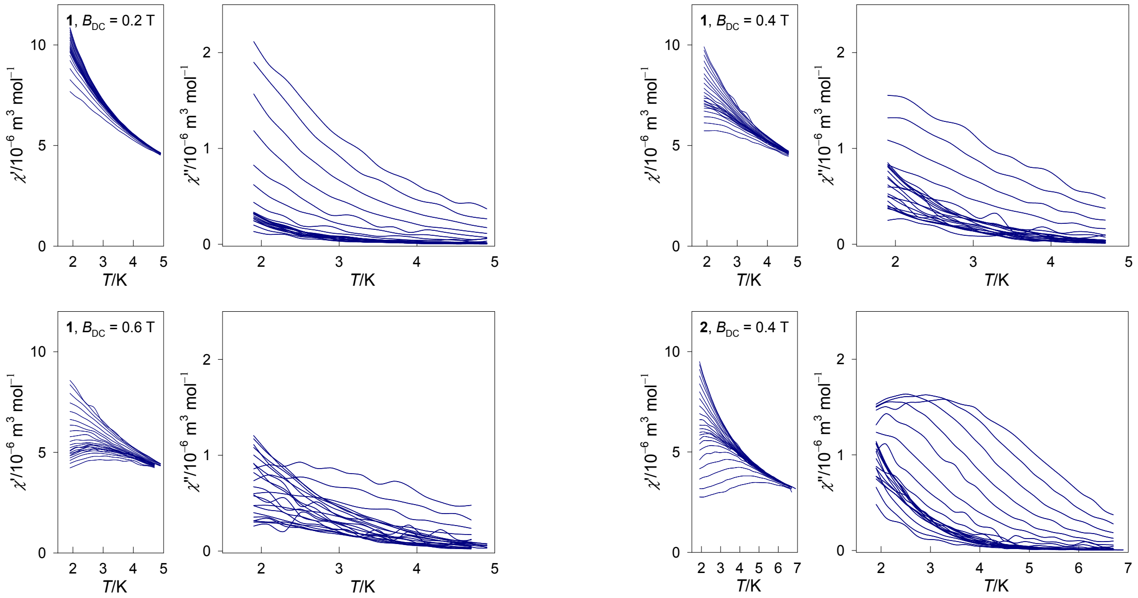

Fig. S3 Temperature dependence of the AC susceptibility components for **1** and **2**.

Fitting of the AC susceptibility data is based upon 44 data points (22 in-phase and 22 out-of-phase) using the formula for the **two-set Debye model**

$$\chi(\omega) = \chi_S + \frac{\chi_{T1} - \chi_S}{1 + (\mathrm{i}\omega\tau_1)^{1-\alpha_1}} + \frac{\chi_{T2} - \chi_{T1}}{1 + (\mathrm{i}\omega\tau_2)^{1-\alpha_2}} \quad \text{or} \quad \chi(\omega) = \chi_S + (\chi_T - \chi_S)\left[\frac{x_1}{1 + (\mathrm{i}\omega\tau_1)^{1-\alpha_1}} + \frac{1 - x_1}{1 + (\mathrm{i}\omega\tau_2)^{1-\alpha_2}}\right]$$

where x_1 is the weight of the first, low-frequency relaxation set (channel, branch). This equation decomposes into two explicit formulae for

a) the in-phase component

$$\chi'(\omega) = \chi_S + (\chi_{T1} - \chi_S)\frac{1 + (\omega\tau_1)^{1-\alpha_1}\sin(\pi\alpha_1/2)}{1 + 2(\omega\tau_1)^{1-\alpha_1}\sin(\pi\alpha_1/2) + (\omega\tau_1)^{2-2\alpha_1}} + (\chi_{T2} - \chi_{T1})\frac{1 + (\omega\tau_2)^{1-\alpha_2}\sin(\pi\alpha_2/2)}{1 + 2(\omega\tau_2)^{1-\alpha_2}\sin(\pi\alpha_2/2) + (\omega\tau_2)^{2-2\alpha_2}}$$

b) the out-of-phase component

$$\chi''(\omega) = (\chi_{T1} - \chi_S)\frac{(\omega\tau_1)^{1-\alpha_1}\cos(\pi\alpha_1/2)}{1 + 2(\omega\tau_1)^{1-\alpha_1}\sin(\pi\alpha_1/2) + (\omega\tau_1)^{2-2\alpha_1}} + (\chi_{T2} - \chi_{T1})\frac{(\omega\tau_2)^{1-\alpha_2}\cos(\pi\alpha_2/2)}{1 + 2(\omega\tau_2)^{1-\alpha_2}\sin(\pi\alpha_2/2) + (\omega\tau_2)^{2-2\alpha_2}}$$ with

the constraint for the isothermal susceptibilities $\chi_{T1} < \chi_{T2}$ in order to get positive contributions from each primitive component. There $x_1 = (\chi_{T1} - \chi_S)/(\chi_{T2} - \chi_S) = (\chi_S - \chi_{T1})/(\chi_S - \chi_{T2})$.

Seven free parameters (χ_S, χ_{T1}, χ_{T2}, α_1, α_2, τ_1, and τ_2) can be fitted reliably by using 44 experimental data points. The functional to be minimized accounts to the relative errors of both susceptibility components

- $F = w \cdot E(\chi') + (1 - w) \cdot E(\chi'')$ with the typical weight $w = 0.07$, or
- $F = E(\chi') \cdot E(\chi'')$ with $E(\chi) = (1/N)\left[\sum_i^N \left|(\chi_i^{\mathrm{e}} - \chi_i^{\mathrm{c}})/\chi_i^{\mathrm{e}}\right|\right]$

The optimization routine refers to the genetic algorithm of D. L. Carroll, Univ. Illinois, Urbana, USA, 1998.

The quality of the fit is expressed by

a) discrepancy factors for the in-phase and out-of-phase susceptibilities $R(\chi')$ and $R(\chi'')$ defined as

$$R(\chi) = \sqrt{\left[\sum_i (\chi_i^{\mathrm{e}} - \chi_i^{\mathrm{c}})^2\right] / \left[\sum_i (\chi_i^{\mathrm{e}})^2\right]}$$

b) by the standard deviation for each optimized parameter; this is given in parentheses, e.g. 12.3(45) means 12.3 ± 4.5 (at 95% probability level).

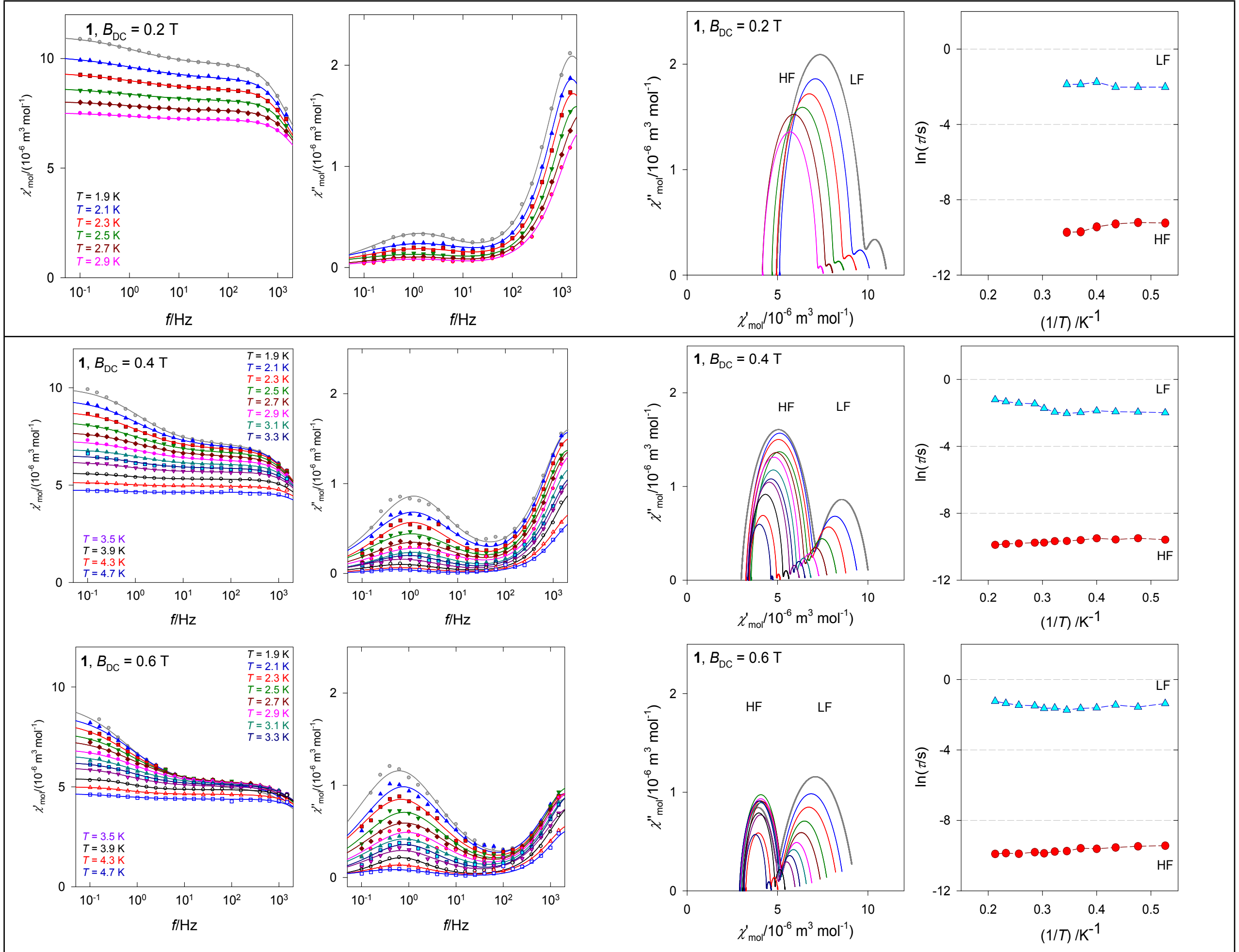

Fig. S4 Frequency dependence of the AC susceptibility components at B_{DC} = 0.2, 0.4 and 0.6 T and at a set of temperatures, along with the fit with the two-set Debye model (left) and Argand and Arrhenius-like plots (right) for **1**.

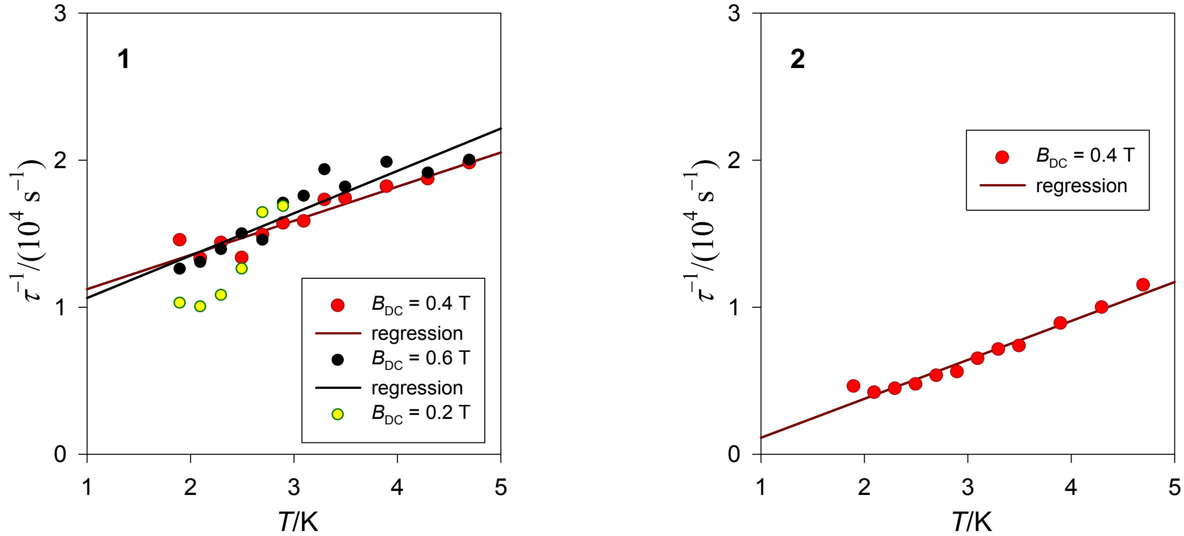

Fig. S5 Temperature dependence of the relaxation time for **1** and **2**. The linear regression confirms the direct mechanism of the relaxation.

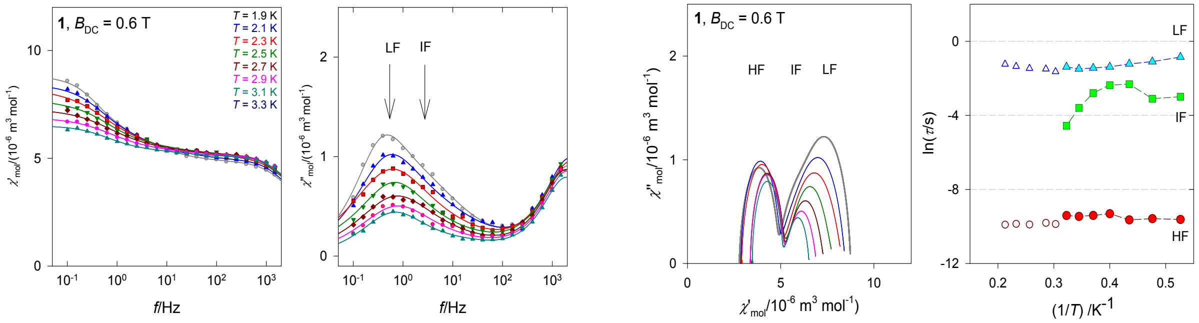

Fig. S6 Frequency dependence of the AC susceptibility components at $B_{DC} = 0.6$ T and fit with the three-set Debye model (left) and Argand and Arrhenius-like plots (right; empty symbols – two-set Debye model) for **1**.

Table S5 Fitted parameters for **1** using the two-set Debye model

a) B_{DC} = 0.2 T

T/K	$R(\chi')$ /%	$R(\chi'')$ /%	χ_S	χ_{LF}	α_{LF}	τ_{LF} /10^{-3} s	χ_{HF}	α_{HF}	τ_{HF} /10^{-6} s	x_{LF}
1.9	0.43	2.1	4.9(2)	6.3(2)	0.41(4)	133(15)	11.0(1)	0.09(1)	97(5)	0.23
2.1	0.59	2.6	5.1(2)	6.2(3)	0.51(7)	133(35)	10.2(1)	0.04(3)	100(6)	0.22
2.3	0.67	2.4	4.9(2)	5.8(3)	0.49(9)	133(45)	9.4(1)	0.03(3)	93(7)	0.20
2.5	0.40	3.2	4.7(2)	5.4(2)	0.54(8)	172(67)	8.7(1)	0.03(2)	79(5)	0.18
2.7	0.26	2.2	4.2(2)	4.6(2)	0.44(6)	153(31)	8.1(3)	0.08(2)	61(4)	0.10
2.9	0.30	3.1	4.2(2)	4.5(2)	0.42(8)	154(41)	7.5(1)	0.07(2)	59(5)	0.09

b) B_{DC} = 0.4 T

T/K	$R(\chi')$ /%	$R(\chi'')$ /%	χ_S	χ_{LF}	α_{LF}	τ_{LF} /10^{-3} s	χ_{HF}	α_{HF}	τ_{HF} /10^{-6} s	x_{LF}
1.9	0.83	6.3	2.9(5)	6.0(6)	0.34(3)	136(9)	10.0(1)	0.16(5)	69(14)	0.44
2.1	0.64	4.4	3.3(3)	5.8(3)	0.38(2)	142(9)	9.5(1)	0.10(3)	75(9)	0.40
2.3	0.67	5.5	3.2(3)	5.2(4)	0.34(3)	145(11)	8.8(1)	0.12(4)	70(10)	0.36
2.5	0.69	4.0	3.5(3)	5.2(3)	0.38(3)	153(15)	8.3(1)	0.08(4)	75(9)	0.35
2.7	0.56	4.5	3.4(3)	4.7(3)	0.38(3)	138(13)	7.8(1)	0.08(3)	67(8)	0.30
2.9	0.62	4.9	3.4(3)	4.4(3)	0.40(4)	130(17)	7.3(1)	0.06(4)	64(9)	0.26
3.1	0.40	4.5	3.5(2)	4.3(2)	0.33(3)	141(13)	6.9(1)	0.06(2)	63(6)	0.24
3.3	0.86	4.8	3.4(4)	4.1(4)	0.31(7)	176(34)	6.5(1)	0.08(5)	58(13)	0.23
3.5	0.37	4.7	3.4(2)	4.0(2)	0.33(5)	232(31)	6.2(1)	0.05(3)	58(7)	0.21
3.9	0.67	6.8	3.4(3)	3.7(3)	0.31(11)	242(75)	5.6(1)	0.03(5)	55(12)	0.14
4.3	0.72	5.0	3.4(3)	3.6(3)	0.24(17)	263(108)	5.1(1)	0.06(5)	54(15)	0.12
4.7	0.68	8.2	3.4(3)	3.5(3)	0.09(24)	298(130)	4.7(1)	0.04(6)	51(16)	0.08

c) B_{DC} = 0.6 T

T/K	$R(\chi')$ /%	$R(\chi'')$ /%	χ_S	χ_{LF}	α_{LF}	τ_{LF} /10^{-3} s	χ_{HF}	α_{HF}	τ_{HF} /10^{-6} s	x_{LF}
1.9	1.1	4.0	2.9(4)	7.3(5)	0.39(2)	255(20)	9.3(1)	0.12(8)	79(23)	0.69
2.1	0.97	6.2	2.9	6.6(1)	0.37(2)	209(13)	8.7(1)	0.11(3)	77(4)	0.64
2.3	0.88	5.0	3.0(4)	6.3(4)	0.39(2)	234(16)	8.4(1)	0.11(7)	72(18)	0.61
2.5	0.90	5.1	2.9(4)	5.6(4)	0.38(3)	200(15)	7.8(1)	0.09(7)	67(17)	0.55
2.7	0.87	4.6	3.1(3)	5.4(4)	0.39(3)	194(16)	7.5(1)	0.10(6)	69(16)	0.52
2.9	0.75	6.8	2.9(4)	4.7(4)	0.36(3)	176(14)	6.9(1)	0.12(6)	59(15)	0.45
3.1	0.72	5.8	3.0(3)	4.5(4)	0.36(3)	198(17)	6.6(1)	0.12(5)	57(14)	0.42
3.3	0.61	7.1	2.9(4)	4.1(4)	0.31(3)	194(16)	6.3(1)	0.12(5)	52(13)	0.35
3.5	0.75	11	3.1(4)	4.1(4)	0.31(5)	224(30)	6.0(1)	0.14(7)	55(19)	0.34
3.9	0.67	7.1	3.1(4)	3.6(4)	0.16(5)	231(24)	5.4(1)	0.08(6)	50(15)	0.22
4.3	0.50	6.5	3.2(2)	3.6(2)	0.21(6)	257(33)	5.0(1)	0.11(5)	52(13)	0.22
4.7	0.56	7.2	3.2(2)	3.4(3)	0.20(9)	290(59)	4.6(1)	0.05(5)	50(14)	0.14

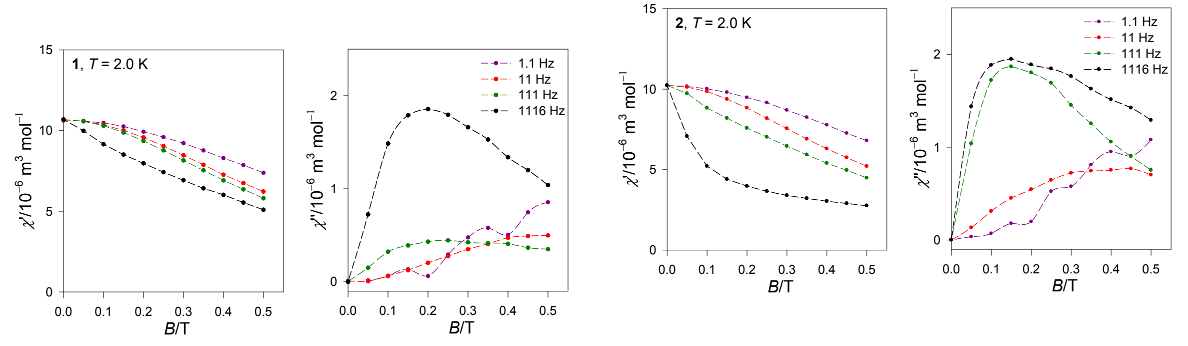

Fig. S7 Comparison of the field dependence of the AC susceptibility components for **1** and **2**.

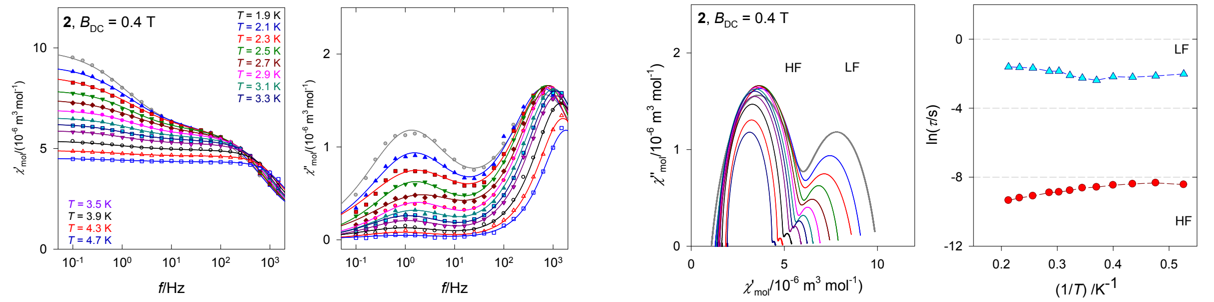

Fig. S8 Frequency dependence of the AC susceptibility components at B_{DC} = 0.4 T and at a set of temperatures, along with the fit with the two-set Debye model (left) and Argand and Arrhenius-like plots (right) for **2**.

Table S6 Fitted parameters for **2** using the two-set Debye model at B_{DC} = 0.4 T

T/K	$R(\chi')$ /%	$R(\chi'')$ /%	χ_S	χ_{LF}	α_{LF}	τ_{LF} /10^{-3} s	χ_{HF}	α_{HF}	τ_{HF} /10^{-6} s	x_{LF}
1.9	0.6	3.2	1.07(14)	5.14(23)	0.35(2)	132(6)	9.95(6)	0.29(2)	217(11)	0.46
2.1	0.7	4.2	1.28(13)	4.50(22)	0.35(2)	118(7)	9.16(6)	0.24(2)	239(11)	0.41
2.3	0.8	3.8	1.46(12)	4.37(23)	0.42(3)	110(8)	8.70(7)	0.19(2)	225(9)	0.40
2.5	0.6	2.1	1.34(8)	3.35(13)	0.32(2)	113(6)	7.93(4)	0.21(1)	211(6)	0.31
2.7	0.7	3.4	1.44(10)	3.25(18)	0.40(3)	92(8)	7.48(5)	0.16(2)	187(6)	0.30
2.9	0.6	2.4	1.43(8)	2.69(11)	0.31(3)	105(7)	6.93(3)	0.16(1)	179(5)	0.23
3.1	0.4	2.1	1.34(7)	2.33(9)	0.31(3)	122(7)	6.55(2)	0.17(1)	154(4)	0.19
3.3	0.4	2.6	1.40(6)	2.23(9)	0.31(3)	156(12)	6.24(2)	0.14(1)	141(4)	0.17
3.5	0.6	3.3	1.53(10)	2.20(12)	0.31(6)	155(21)	5.90(3)	0.12(1)	136(5)	0.15
3.9	0.5	3.7	1.64(9)	2.12(12)	0.39(7)	186(42)	5.39(4)	0.07(2)	113(5)	0.13
4.3	0.5	3.1	1.85(8)	2.12(9)	0.32(9)	194(48)	4.90(3)	0.04(1)	100(4)	0.09
4.7	0.6	3.5	1.94(11)	2.12(14)	0.41(17)	200(123)	4.52(4)	0.01(2)	87(5)	0.07

Table S7 The primary ligand, composition,[a] coordination environment and glossary of SIM properties of previously reported Co^{II} SIMs from imino-phenol ligands.

Primary ligand	**Composition of the SIM**	**Coordination environment of Co^{II}**	**Glossary of magnetic properties**	**References**
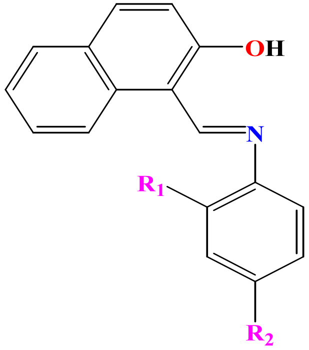 HL^A: R^1 = H, R^2 = Br. HL^B: R^1 = Ph, R^2 = H.	$[Co^{II}(L^A)_2]$ (**I**). $[Co^{II}(L^A)_2]$ (**II**).	$CoN(imine)_2O(phenoxo)_2$; Tetracoordinated; Distorted tetrahedral.	**I**: $D = -36.7$ cm^{-1}; $U_{eff} = 36$ cm^{-1} at 0.04 T. **II**: $D = -39.8$ cm^{-1}; $U_{eff} = 43$ cm^{-1} at 0.04 T.	1
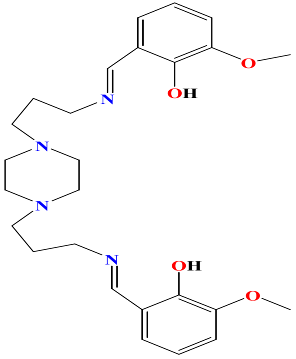 H_2L^C	$[Co^{II}L^C]$ (**III**)	$CoN(imine)_2N(amine)_2O(phenoxo)_2$; Hexacoordinated; Distorted trigonal prism.	$D = -41$ cm^{-1}; $U_{eff} = 56.65$ cm^{-1} at 0.12 T.	2

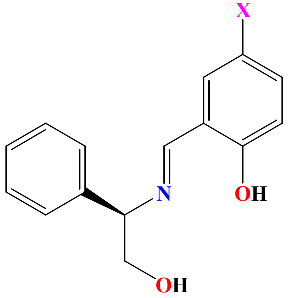 H_2L^D: X = H. H_2L^E: X = ^{t}But. H_2L^F: X = Br. H_2L^G: X = NO_2.	$[Cation][Co^{II}Co^{III}_3(L^{D/E/F/G})_6]$ ^{b} (**IV–XI**)	CoO(μ-phenoxo)$_6$; Hexacoordinated; Distorted trigonal prism.	*D*: in the range from –28.8 to –115 cm^{-1}; U_{eff} = 26.6 – 102.8 cm^{-1} at zero field and 28.7 – 113.3 cm^{-1} at 0.15 T.	3, 4
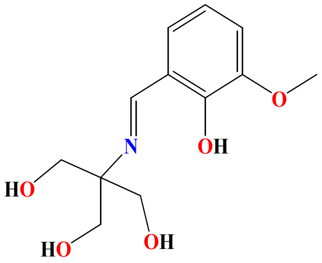 H_4L^H	$[Co^{III}Co^{II}(H_2L^H)_2(H_2O)Cl]$ (**XII**). $[Co^{III}Co^{II}(H_2L^H)_2(H_2O)Br]$ (**XIII**). $[Co^{III}Co^{II}(H_2L^H)_2(H_2O)(OAc)]$ (**XIV**)	CoO(μ-alkoxo)$_2$O(alcoholic OH)2O(H2O)Y] (Y = Cl$^-$, Br$^-$, OAc$^-$) Hexacoordinated; Distorted octahedral.	**XII**: *D* = –7.4 cm^{-1}; U_{eff} = 7.9 cm^{-1} at 0.1 T. Two relaxation pathways. **XIII**: *D* = –9.7 cm^{-1}; U_{eff} = 14.5 cm^{-1} at 0.1 T. Two relaxation pathways. **XIV**: *D* = 145 cm^{-1}; U_{eff} = 11.2 cm^{-1} at 0.1 T. Two relaxation pathways.	5, 6

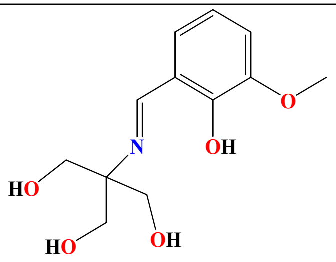 H_4L^H	$[\mathrm{Co^{III}Co^{II}(H_2L^H)_2(H_2O)_2}]$ $[\mathrm{Co^{III}Co^{II}(H_2L^H)_2(H_2O)}(m\text{-}\mathrm{phth})]$ ^{c}(**XV**)	$\mathrm{CoO(\mu\text{-}alkoxo)_2O(alcoholic\ OH)_2O(H_2O)O(Y)]}$ ($Y = H_2O$ for the cation and *m*-phth for the anion) Hexacoordinated; Distorted octahedral.	$\lvert D \rvert = 54.7\ \mathrm{cm^{-1}}$; $D(\mathrm{theo}) = -62.4\ \mathrm{cm^{-1}}$ for the cation and $-95.8\ \mathrm{cm^{-1}}$ for the anion. $U_{\mathrm{eff}} = 19.0\ \mathrm{cm^{-1}}$ at 0.1 T.	7
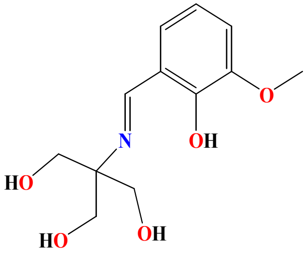 H_4L^H	$[\{\mathrm{Co^{III}Co^{II}(H_2L^H)_2(H_2O)}\}_2(\mathrm{ppda})]$ ^{d} (**XVI**)	$\mathrm{CoO(\mu\text{-}alkoxo)_2O(alcoholic\ OH)_2(H_2O)O(ppda)}$. Hexacoordinated; Distorted octahedral.	$\lvert D \rvert = 60.8\ \mathrm{cm^{-1}}$; $D(\mathrm{theo}) = -101.9\ -95.8\ \mathrm{cm^{-1}}$. $U_{\mathrm{eff}} = 32.3\ \mathrm{cm^{-1}}$ at 0.1 T.	7
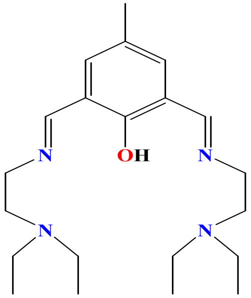 HL^1	$[\mathrm{Co^{III}(N_3)_2L^1(\mu_{1,1}\text{-}N_3)Co^{II}(N_3)}]$ (**1**)	CoO(μ-phenoxo)N(imine)N(amine)N(mu1,1-azido)N(terminal azido). Pentacoordinated; Distorted square pyramidal.	$D = 40\ \mathrm{cm^{-1}}$; $D(\mathrm{theo}) = 42.4\ \mathrm{cm^{-1}}$. Two relaxation pathways.	This work

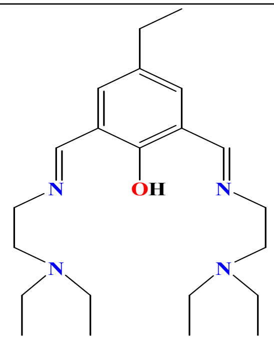 HL^2	$[Co^{III}(N_3)_2L^2(\mu_{1,1}\text{-}N_3)Co^{II}(N_3)]$ (**2**)	CoO(μ-phenoxo)N(imine)N(amine)N(mu1,1-azido)N(terminal azido). Pentacoordinated; Distorted square pyramidal.	*D*(theo) = 45.7 cm^{-1}. Two relaxation pathways.	This work

[a] Excluding solvent of crystallization. [b] Cations are Protonated triethylamine, 1,8-diazabicyclo[5.4.0]undec-7-ene and N,N-diisopropylethylamine, and tetrabutyylammonium. [c] *m*-phth = monodeprotonated phthalic acid. [d] ppda = 1,4-phenylenediacrylate.

References

(1) S. Ziegenbalg, D. Hornig, H. Görls and W. Plass, *Inorg. Chem.*, 2016, 55, 4047.

(2) Y. Peng, T. Bodenstein, K. Fink, V. Mereacre, C. E. Ansona and A. K. Powell, *Phys. Chem. Chem. Phys.*, 2016, **18**, 30135;

(3) Y.-Y. Zhu, C. Cui, Y.-Q. Zhang, J.-H. Jia, X. Guo, C. Gao, K. Qian, S.-Da Jiang, B.-W. Wang, Z.-M. Wanga and S. Gao, *Chem. Sci.*, 2013, **4**, 1802;

(4) Y.-Y. Zhu, Y.-Q. Zhang, T.-T. Yin, C. Gao, B.-W. Wang and S. Gao, *Inorg. Chem.*, 2015, **54**, 5475;

(5) V. Chandrasekhar, A. Dey, A. J. Mota and E. Colacio, *Inorg. Chem.*, 2013, **52**, 4554;

(6) E. A. Buvaylo, V. N. Kokozay, O. Yu. Vassilyeva, B. W. Skelton, A. Ozarowski, J. Titiš, B. Vranovičová and R. Boča, *Inorg. Chem.*, 2017, **56**, 6999;

(7) S. Manna, A. Bhunia, S. Mistri, J. Vallejo, E. Zangrando, H. Puschmann, J. Cano and S. C. Manna, *Eur. J. Inorg. Chem.*, 2017, 2585.